UDC 621.372; 616.12-073.7

N. Tulyakova, O. Trofymchuk

ADAPTIVE MYRIAD FILTERING ALGORITHMS FOR REMOVAL OF NONSTATIONARY NOISE IN ELECTROOCULOGRAMS

Nataliya Tulyakova

Institute of Applied Physics NAS of Ukraine, Sumy,
orcid: 0000-0002-9158-8967

nataliyatulyakova@google.com

Oleksandr Trofymchuk

Institute of Telecommunications and Global Information Space NAS of Ukraine, Kyiv,
orcid: 0000-0003-3358-6274

trofymchuk@nas.gov.ua

Suppressing nonstationary noise present in biomedical signals is important to provide high-quality diagnoses. Nonstationary noise is difficult for removing due to its time-varying and previously unknown characteristics. The application of linear filtering to the electrooculograph (EOG) signals leads to the smoothing of diagnostically important rapid changes in a signal caused by saccadic eye movements. In this respect, for processing edges and other discontinuous transitions, nonlinear filters based on robust estimators are more appropriate. The paper introduces novel adaptive algorithms for real-time nonlinear filtering of nonstationary noise in EOG signal with a noise- and signal-dependent filter switching, which is more appropriate for processing a local vicinity of the current input signal sample. One of the algorithms is based on myriad filters and sub-filter weighted FIR (which inite Impulse Responce) myriad hybrid filters. It suggests replacing the median with a myriad operation, calculated by Newton′s numerical technique with adaptive switching of window length and linearity parameter settings. The other algorithm adaptively switches sub-filter weighted FIR median hybrid and averaging filters with different window lengths, offering simpler calculations and high-speed performance. These algorithms do not require time for filter parameters modification and their exact tuning during real-time signal processing and a prior knowledge of the signal model and noise variance. Numerical simulations were conducted to evaluate the filtering quality based on criteria of mean-square error and signal-to-noise ratio for a model signal under different levels of Gaussian noise. The achieved results show good performance and algorithm high quality for suppression of nonstationary noise in EOG. The myriad type adaptive algorithm prevails over the median in effectiveness but requires a numerical technique for cost function minimization, however, myriad filtering real-time implementation is possible with utilization of high-speed computers. Suggested adaptive algorithms significantly improve the efficiency of nonadaptive filters.

Keywords: electrooculographic signals, nonstationary noise, real time adaptive filtering.

Introduction

Electrooculographic (EOG) signals arise from the electrically charged eyes described with an equivalent dipole located within the eye with the positive charge in the cornea and the negative one in the retina [1]. The recording of eye movement biomedical signals is a relatively simple and nonintrusive procedure that does not cause discomfort or affect vision. It can be conducted over extended periods, both during the day and at night, and can even be performed remotely. The necessary equipment (electrodes, direct current amplifiers) for recording the electrical activity around the eye is cost-effective and affordable. The signals registration does not violate the natural conditions of oculomotor activity. These biomedical signals help diagnose the diseases and disorders of the optokinetic and central nervous systems, brain, vision, as well as the influence of medicinal and narcotic drugs, alcohol, states of fatigue, etc. [2]. As well, the registration of EOG signals can be used for the eye movements artifacts subtraction in the electroencephalograms [3, 4].

Nonstationary noise contaminating biomedical signals is difficult for removing because its time-varying and previously unknown characteristics. Therefore, designing adaptive algorithms to attenuate nonstationary noise is an important task to be performed. For EOG signal processing it is essential to preserve sharp («step-like») changes caused by saccadic eye movements, which are smoothed by linear filtering [5]. The maximum speed of saccades, which is a very important diagnostic parameter [2, 6], can be significantly distorted as a result of smoothing. In this respect, the median [5–7], hybrid median [8–11], and myriad [12–16] filters, which effectively attenuate undesirable noise, but retain diagnostic information in the step-like pulses, are more appropriate. However, linear averaging high-effectively suppresses white noise on the constant and linear parts of a signal [5, 17–19]. Therefore, the signal-adapting processing with combining advantages of nonlinear and linear filters is reasonable. Such adaptive real-time processing can be provided by the so-called «locally-adaptive» algorithms of nonlinear filtering in a data sliding window for suppression noise in processes with different a priori unknown behavior of the information component [20–22]. These algorithms involve the so-called «local activity indicators» (LAIs) calculated for each signal sample, which simplystically estimate the local signal behavior to switch adaptively a more appropriate filter from the fixed set of relevant filter settings for processing the neighborhood of a current i-th signal sample.

For nonstationary noise removal in the signals with different behavior of an informative component, in particular for electrocardiographic and electronystagmographic biomedical signal processing, the locally-adaptive algorithms with a noise- and signal-dependent switching filter settings were introduced [23–25]. In these algorithms, a filter set with more relevant window lengths is adaptively switched according to the pre-estimated noise level and a more appropriate filter from the selected filter set is chosen by LAIs comparisons for processing a vicinity of the current input signal sample. The noise- and signal-dependent locally-adaptive filters prove to be efficient in preserving the rapid changes within the signal by refraining from filtering at very low noise levels. They also minimize dynamical errors resulting from filtering with small and medium window lengths at low and mean noise levels. Furthermore, these filters enhance noise attenuation by increasing the filter window length. The noise- and signal-dependent flexible window length adjustment during processing with none-filtering in case of noise absence initially was proposed in dynamic approximating algorithms [26–29], which apply linear Savitzky and Golay approximation [30], leading to sharp edge smoothing. In contrast to these algorithms [26–29, 31–33], the proposed locally-adaptive algorithms with «hard» filter settings switching [23–25, 34–36] allow filtering with different properties, including nonlinear and linear estimation, to preserve sharp signal changes and other discontinuous transitions in a signal while ensuring efficient noise attenuation, in particular on linear sections of the signal.

The study is aimed to develop noise- and signal-adapting nonlinear filtering algorithms for the purpose of removing nonstationary noise in EOG signals. The performance of these algorithms will be evaluated and compared with other nonlinear filters that have been effectively used for similar signals. The paper has four sections. Introduction presents the reasons for development of adaptive nonlinear filtering algorithms for nonstationary noise removal in the biomedical signals of eye movements. Section 1 describes the methods used in the study. Subsection 1.1 describes some reference nonlinear filters which are effective for the considered biomedical signals and the suggested noise- and signal-adapting algorithms for nonstationary noise real-time filtering. Subsection 1.2 shows the way the experimental results were obtained and applied model signal, it also states the criteria for filtering quality assessment. In subsection 1.3, the adaptive filter parameters are specified. Section 2 performs some numerical experiments and discusses the efficiency of the adaptive filtering algorithms introduced. Subsection 2.1 presents the statistical estimates of filter efficiency obtained by numerical simulations. Subsection 2.2 illustrates the input signal with highly nonstationary noise and the corresponding output signals and residual noise after filtering, and the plots, displaying LAIs and adaptable parameters behaviour.

1. Methods

1.1. Filters under study.

Nonadaptive filters. The following nonlinear filters have been used for comparisons:

Median filter [5–7, 17, 18] that is the optimal M-estimate (maximum likelihood) for the exponential probability density function (PDF) of random sample x_i:

$$y_i^{Med} = median\{x_1, \ldots, x_i, \ldots, x_{Ni}\}, \quad (1)$$

where $\{x_1, \ldots, x_i, \ldots, x_{Ni}\}$ are input signal samples within the sliding window with length N. The median filter is robust estimator with highly nonlinear properties [17, 18].

Myriad filter [12–16] that is optimal M-estimate for the Cauchy PDF:

$$y_i^{Myr} = myriad\{x_1, \ldots, x_i, \ldots, x_N; K_i\} = \arg\min_{\beta} \sum_{i=1}^{N} \log\,[K_i^2 + w_i(x_i - \hat{\beta})^2], \quad (2)$$

where $\{x_1, \ldots, x_i, \ldots, x_{Ni}\}$ are input signal samples within the sliding window with length N; K_i is the linearity parameter of the myriad estimator, $K_i > 0$; $\hat{\beta}$ is the Cauchy PDF location estimate by the samples of a random variable $\{x_i\}|_{i=1}^{N}$.

The myriad filter in the nonlinear operation mode (the linearity parameter K is close to zero) has higher nonlinearity than the median filter, however, it requires more complex calculations. The nonlinearity of myriad filter properties depends on the linearity parameter K. The myriad filter performs highly nonlinear properties (in particular, concerning step response [37, 38] at small K values and tends to linear averaging when K increases [12–16].

Sub-filter weighted FIR (with finite impulse response) median hybrid filter [10, 11]:

$$y_i^{SWFMH} = median\{\hat{x}_{fw_i}^1,\ 2\Diamond\hat{x}_{fw_i}^0, x_i,\ 2\Diamond\hat{x}_{bw_i}^0, \hat{x}_{bw_i}^1\},, \quad (3)$$

where x_i is the center element inside the filter window; $\hat{x}_{fw_i}^0 \sum_{j=1}^{k} x_{i-j} / k$, $\hat{x}_{bw_i}^0 = \sum_{j=1}^{k} x_{i+j} / k$ are the outputs of the FIR sub-filters which predict a current sample of the signal described by the zero-order polynomial (level estimates); $\hat{x}_{fw_i}^1 = \sum_{j=1}^{k} h_j\, x_{i-j}$,

$\hat{x}^1_{bw_i} = \sum_{j=1}^{k} h_j\, x_{i+j}$ are the outputs of the FIR sub-filters which predict a current output signal described by the first order polynomial (ramp estimates); the zeroth and the first order FIR predictors which estimate output signal from *k* past («fw» denotes forward prediction) and *k* future input signal samples («bw» denotes backward prediction) related to the current *i*-th sample within the sliding window with length $N = 2k+1$; $h_j = (4k - 6j + 2)/(k(k-1))$ are the FIR coefficients for first order prediction, $j = 1, ..., k$ [8–11, 39]; $\Diamond$ is nonlinear weighting operator (duplication of an element by a given number of times).

Sub-filter weighted FIR median hybrid filter preserves step and ramp edge, simultaneously suppressing noise in their vicinities with high efficiency. The first-order FIR sub-filters ensure the triangular signals preservation, while the standard FIR median hybrid filter [8–11, 17] introduces specific errors in extrema regions. By adding weights to the zeroth order FIR sub-filters, the noise attenuation in the vicinity of the edges is increased [10, 11].

- Sub-filter weighted FIR hybrid filter used myriad operation instead of median [38]:

$$y_i^{SWFMH} = myriad\{\hat{x}^1_{fw_i},\ 2\Diamond\hat{x}^0_{fw_i}, x_i, 2\Diamond\hat{x}^0_{bw_i}, \hat{x}^1_{bw_i}\}, \tag{4}$$

A myriad will be estimated from seven points in the window only; hence, that does not cause a significant computational cost increase. The proposed median operation replacement by myriad improves filtering quality [38].

Noise- and signal-adapting nonlinear filtering algorithms. EOG signal processing can be performed with a noise- and signal-dependent algorithm based on myriad filters and weighted FIR myriad hybrid filters with adaptive switching of window length N and linearity parameter Ka controlling filter nonlinearity:

$$y_i = \begin{cases} \begin{cases} y_i^{Myr_{3,1}(N_{3,1}, Ka_{3,1})}, \text{if } (\hat{n}_i = 1) \text{ and } ((r_i^f > th_i^f) \text{ or } (|Q_{Zi}^f| < t_{Z1})), \\ y_i^{Myr_{2,1}(N_{2,1}, Ka_{2,1})}, \text{if } (\hat{n}_i = 1) \text{ and } (r_i^f \le th_i^f) \text{ and } (|Q_{Zi}^f| \le t_Z), \\ x_i, \text{ if } (\hat{n}_i = 1) \text{ and } (r_i^f \le th_i^f) \text{ and } (|Q_{Zi}^f| > t_Z); \end{cases} \\ \begin{cases} y_i^{Myr_{3,2}(N_{3,2}, Ka_{3,2})}, \text{if } (\hat{n}_i = 2) \text{ and } ((r_i^f > th_i^f) \text{ or } (|Q_{Zi}^f| < t_{Z1})), \\ y_i^{Myr_{2,2}(N_{2,2}, Ka_{2,2})}, \text{if } (\hat{n}_i = 2) \text{ and } (r_i^f \le th_i^f) \text{ and } (|Q_{Zi}^f| \le t_Z), \\ y_i^{Myr_{1,2}(N_{1,2}, Ka_{1,2})}, \text{ if } (\hat{n}_i = 1) \text{ and } (r_i^f \le th_i^f) \text{ and } (|Q_{Zi}^f| > t_Z); \end{cases} \\ \ldots \\ \begin{cases} y_i^{SWFMHmyr_{3,j}(N_{3,j}, Ka_{3,j})}, \text{if } (\hat{n}_i = j) \text{ and } ((r_i^f > th_i^f) \text{ or } (|Q_{Zi}^f| < t_{Z1})), \\ y_i^{SWFMHmyr_{2,j}(N_{2,j}, Ka_{2,j})}, \text{if } (\hat{n}_i = j) \text{ and } (r_i^f \le th_i^f) \text{ and } (|Q_{Zi}^f| \le t_Z), \\ y_i^{SWFMHmyr_{1,j}(N_{1,j}, Ka_{1,j})}, \text{if } (\hat{n}_i = j) \text{ and } (r_i^f \le th_i^f) \text{ and } (|Q_{Zi}^f| > t_Z); \end{cases} \\ \ldots \\ \begin{cases} y_i^{SWFMHmyr_{3,L}(N_{3,K}, Ka_{3,L})}, \text{if } (\hat{n}_i = L) \text{ and } ((r_i^f > th_i^f) \text{ or } (|Q_{Zi}^f| < t_{Z1})), \\ y_i^{SWFMHmyr_{2,L}(N_{2,L}, Ka_{2,L})}, \text{if } (\hat{n}_i = L) \text{ and } (r_i^f \le th_i^f) \text{ and } (|Q_{Zi}^f| \le t_Z), \\ y_i^{SWFMHmyr_{1,L}(N_{1,L}, Ka_{1,L})}, \text{if } (\hat{n}_i = L) \text{ and } (r_i^f \le th_i^f) \text{ and } (|Q_{Zi}^f| > t_Z); \end{cases} \end{cases} \tag{5}$$

where x_i is an input signal; $y_i^{Myr_{k,j}(N_{k,j},Ka_{k,j})}$, $k=1,...,3$, $j=1,...,L_1$, are outputs of myriad filters to be applied at low noise levels ($\hat{n}_i=1,...,L_1$); $y_i^{SWFMHmyr_{k,j}(N_{k,j},Ka_{k,j})}$, $k=1,...,3$, $j=L_1+1,...,L$, are outputs of sub-filter weighted FIR myriad hybrid filters to be applied at higher noise levels $\hat{n}_i=L_1+1,...,L$); $N_{1j}\le N_{2j}\le N_{3j}$ are window lengths for j-th filter set; $Ka_{1j}\le Ka_{2j}\le Ka_{3j}$ are parameters which set different nonlinearities to the myriad estimate, $j=1,...,L$; $\hat{n}_i$ is a flag variable that defines different noise levels; r_i^f, th_i^f, $|Q_{Zi}^f|$ are LAIs, as which the filtered Hampel identifiers [40, 41] and the absolute value of Z-parameter quasi-range [21, 22] are used; t_{Z_1}, t_Z are the low and the upper thresholds for $|Q_{Zi}^f|$ comparison.

Hampel filter [40, 41] identifiers r_i, th_i can be described as

$$r_i=|x_i-m_i|,\ th_i=tS_i^{MAD},$$
$$S_i^{MAD}=1,4826\ median\{|x_1-m_i|,\ |x_2-m_i|,\ldots,|x_N-m_i|\}, \quad (6)$$

where x_i and m_i are the center sample and median of the input samples $\{x_j\}|_{j=1}^N$ within a sliding window of length N; S_i^{MAD} is a median absolute deviation (MAD), which is a robust estimate of the scale (spread width of the PDF of a random variable), 1,4826 is a coefficient used for Gaussian PDF [12]; t is a fixed threshold; $|\cdot|$ denotes an absolute value.

Z-parameter and its quasi-range Q_{Z_i} can be described as

$$Z_i=\sum_{j=-(N_Z-1)/2}^{(N_Z-1)/2}(y_{i-j}^f-x_{i-j})\Big/\sum_{j=-(N_Z-1)/2}^{(N_Z-1)/2}|y_{i-j}^f-x_{i-j}|, \quad (7)$$

where x_{i-j}, y_{i-j}^f are input and pre-filtered samples, respectively; N_Z is a window length;

$$Q_{Z_i}=Z_i^{(q)}-Z_i^{(p)},\ q+p=N_Q+1,\ q>p, \quad (8)$$

where q and p are the order statistics ranks of the sorted set $Z_i^{(1)}\le\ldots$ $\ldots\le Z_i^{(j)}\le\ldots\le Z_i^{(N_Q)}$ within a sliding window $\{Z_{i-(N_Q-1)/2},\ldots,Z_i,\ldots,Z_{i-(N_Q+1)/2}\}$, containing Z-parameter values; N_Q is the length of this window.

A flag variable for preliminary noise level estimation can be written as

$$\hat{n}_i=\begin{cases}1,\text{ if }(r_i^f>th_i^f)\text{ and }(|Q_{Zi}^f|\le t_{Z_1})\text{ and }(r_i^f<\eta_1),\\ 2,\text{ if }(r_i^f>th_i^f)\text{ and }(|Q_{Zi}^f|\le t_{Z_1})\text{ and }(\eta_1\le r_i^f<\eta_2),\\ \ldots\\ j,\text{ if }(r_i^f>th_i^f)\text{ and }(|Q_{Zi}^f|\le t_{Z_1})\text{ and }(\eta_{j-1}\le r_i^f<\eta_j),\\ \ldots,\\ L,\text{ if }(r_i^f>th_i^f)\text{ and }(|Q_{Zi}^f|\le t_{Z_1})\text{ and }(r_i^f\ge\eta_{L-1});\end{cases}, \quad (9)$$

where r_i^f, th_i^f, $Q_{Z\,i}^f$ are filtered values of Hampel identifiers and *Z*-parameter quasi-range, used as LAIs; t_{Z_1} is the low threshold for *Z*-parameter; η_1, η_2, …, η_{L-1} are thresholds for noise levels estimation; L is the number of estimated noise levels.

It is proposed to simply estimate the noise level by comparison a LAI with given thresholds. «This estimation is performed on the slowly alternating signal part when there is the condition $(r_i^f > th_i^f)$ and $(|Q_{Z\,i}^f| < t_{Z_1})$». A flag variable conventionally defines different noise levels from 1 — «very low» to L — «very high», for which there is a reason to switch the filters with enlarged (in case of increasing noise variance) or diminished (in case of decreasing noise variance) window lengths.

When the computational complexity of signal processing algorithms is significantly limited, not allowing myriad filtering, the locally-adaptive algorithm for adaptive switching of sub-filter weighted FIR median hybrid filters (3), due to their high quality in the edges vicinities, and simple averaging filters, which provide high degree of noise suppression on the linear signal parts, with different window lengths is suggested:

$$y_i = \begin{cases} \begin{cases} y_i^{AF_{3,1}(N_{3,1})}, \textit{ if } (\hat{n}_i = 1) \textit{ and } ((r_i^f > th_i^f) \textit{ or } (|Q_{Z\,i}^f| < t_{Z1})), \\ y_i^{SWFMH_{2,1}(N_{2,1})}, \textit{ if } (\hat{n}_i = 1) \textit{ and } (r_i^f \le th_i^f) \textit{ and } (|Q_{Z\,i}^f| \le t_Z), \\ x_i, \textit{ if } (\hat{n}_i = 1) \textit{ and } (r_i^f \le th_i^f) \textit{ and } (|Q_{Z\,i}^f| > t_Z); \end{cases} \\ \dots \\ \begin{cases} y_i^{AF_{3,j}(N_{3,j})}, \text{ if } (\hat{n}_i = j) \text{ and } ((r_i^f > th_i^f) \text{ or } (|Q_{Z\,i}^f| < t_{Z1})), \\ y_i^{SWFMH_{2,j}(N_{2,j})}, \text{ if } (\hat{n}_i = j) \text{ and } (r_i^f \le th_i^f) \text{ and } (|Q_{Z\,i}^f| \le t_Z), \\ y_i^{SWFMH_{1,j}(N_{1,j})}, \text{ if } (\hat{n}_i = j) \text{ and } (r_i^f \le th_i^f) \text{ and } (|Q_{Z\,i}^f| > t_Z); \end{cases} \\ \dots \\ \begin{cases} y_i^{AF_{3,L}(N_{3,L})}, \text{ if } (\hat{n}_i = L) \text{ and } ((r_i^f > th_i^f) \text{ or } (|Q_{Z\,i}^f| < t_{Z1})), \\ y_i^{SWFMH_{2,L}(N_{2,L})}, \text{ if } (\hat{n}_i = L) \text{ and } (r_i^f \le th_i^f) \text{ and } (|Q_{Z\,i}^f| \le t_Z), \\ y_i^{SWFMH_{1,L}(N_{1,L})}, \text{ if } (\hat{n}_i = L) \text{ and } (r_i^f \le th_i^f) \text{ and } (|Q_{Z\,i}^f| > t_Z); \end{cases} \end{cases} \quad (10)$$

«where x_i is an input signal; $y_i^{SWFMH_{1,j}(N_{1,j})}$, $y_i^{SWFMH_{2,j}(N_{2,j})}$, $j = 1, ..., L$, are outputs of sub-filter weighted FIR median hybrid filters (3)»; $y_i^{AF_{3,j}(N_{3,j})}$ are outputs of simple averaging filters; N_{1j}, N_{2j}, N_{3j} ($N_{1j} \le N_{2j}$) are window lengths of *j*-th filter set.

1.2. Numerical simulation algorithm. Statistical estimates of filter efficiency were obtained using numerical simulation (via Monte Carlo analysis) according to the following algorithm [17]: 1) a test «clean» signal is formed; 2) a noise with given characteristics is randomly generated and superimposed with the test signal; 3) a filtering algorithm with specified parameters is applied; 4) performance indicators are calculated and fixed; 5) the filtering is repeated many times for a large number of signal realizations with random noise, while the performance indicators are averaged.

The commonly filter efficiency estimation criteria of minimum mean square error (MSE) and maximum signal-to-noise ratio (SNR) are applied to evaluate the

filtering quality [17]. Statistical estimates of filter efficiency accordingly to the MSE (χ) and SNR (q) criteria are expressed as

$$\chi = \sum_{j=1}^{N_R} \left(\sum_{i=i_1}^{i_2} (y_i^f - s_i)^2 / I \right) / N_R , \tag{11}$$

where y_i^f is the output of the evaluated filter of the i-th sample; s_i is a «clean» signal; I is the length of signal realization; N_R is the number of noisy test signal realizations for statistical averaging:

$$q = \sum_{j=1}^{N_R} 10 \lg(p_s / p_n / N_R , \; p_s = \sum_{i=1}^{I} (s_i - \bar{s})^2 / I ,$$

$$p_n = \sum_{i=1}^{I} (y_i^f - s_i)^2 / I , \; \bar{s} = \sum_{i=1}^{I} s_i / I , \tag{12}$$

where p_s and p_n are signal and noise powers.

A piecewise signal with vertical step lines simulated model EOG signal (Fig. 1, *a*), which is similar to the EOG signals sampled at 100 Hz (Fig. 1, *b*) was taken as a «clean» signal to be used in numerical simulation. This model signal is somewhat «ideal»: it is assumed that the upper-frequency spectrum limitation is absent and, therefore, a high-frequency noise is present in the test signal since the step changes were simulated as vertical lines. Similar real signals are recorded in simple conditions when the examined person is looking to the left and to the right according to the rhythm given by alternating LEDs (light-emitting diodes), which light up for a period of 1; 0,5 or 0,25 seconds, that allows determination of the eyeball angular velocity.

The suggested nonlinear locally-adaptive algorithms are applied to the signals sampled at low frequencies when adaptive switching of not large windows is reasonable. A filter with a large window length is required to suppress high-frequency fluctuations in the signals with a high sampling rate; in this case, nonlinear trend detection algorithms of the median or myriad types are efficient [42–44].

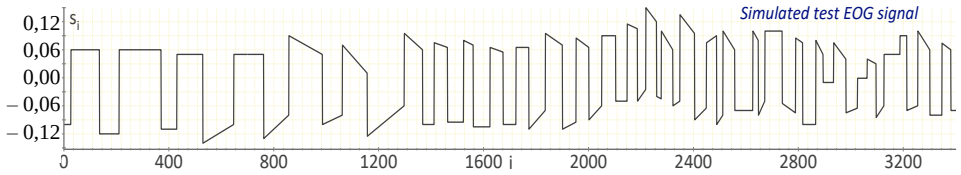

a

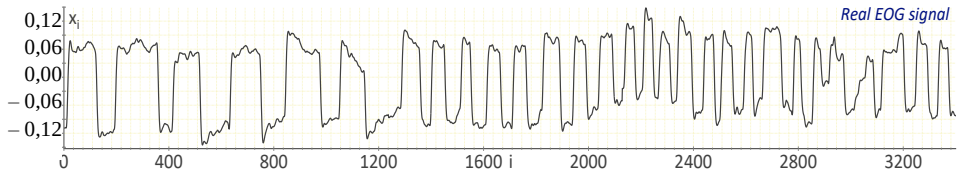

b

Fig. 1

1.3. Parameter settings for considered algorithms. For the proposed locally-adaptive filters, the suitable filter parameters were chosen by numerical simulations for the considered test signals (Fig. 1) according to a minimum of MSE (11) or a maximum of SNR (12) at the filter output in the presence of the Gaussian noise with a zero mean

and different variance. The proposed EOG processing myriad algorithm (5) and its modification [23–25] with selective re-filtering (when the noise reaches a not very low level, when flag variable $\hat{n}_i$ (9) greater than 2) are denoted as ASWFmyr1P, ASWFmyr2P, and the median algorithm (10) and its mentioned modification as ASWFmed1P and ASWFmed2P.

The following parameters were chosen for LAIs calculations: for Hampel parameters r_i, th_i (6) the window with length $N = 21$ and threshold $t = 0.6$ are used, these parameters are smoothed by averaging filters with windows $N_1 = 23$ and $N_2 = 15$, respectively; for *Z*-parameter (3), the input signal is pre-filtered by myriad filter (2) with parameters $N = 21$, $K = 0{,}03$, for *Z*-parameter (7) and its quasi-range Q_{Z_i} (8) calculations the windows $N_Z = 11$ and $N_Q = 15$ are used, the low and upper thresholds are $t_{Z_1} = 0{,}2$; $t_Z = 0{,}4$, the Q_{Z_i} values are processed by median filter with window $N_3 = 11$. For myriad adaptive filters ASWFmyr1P and ASWFmyr2P (5), the noise levels are estimated by the following thresholds: $\eta_1 = 0{,}001$; $\eta_2 = 0{,}002$; $\eta_3 = 0{,}005$; $\eta_4 = 0{,}01$; $\eta_5 = 0{,}03$; $\eta_6 = 0{,}08$; $\eta_7 = 0{,}15$. Accordantly, in the first three filter sets, the myriad filters based on Newton's numerical technique [45, 46] with an excellent step response at low noise levels are adaptively switched, and in the next four filter sets the sub-filter weighted FIR myriad hybrid filters, which preserve edges and strongly suppress noise in their vicinities, are applied. The correspondent parameter sets for adaptive switching are as follows: { $N_{21} = N_{31} = 17$, $Ka_{21} = Ka_{31} = 0{,}03$}, { $N_{12} = 9$, $Ka_{12} = 0{,}01$; $N_{22} = N_{32} = 19$, $Ka_{22} = Ka_{32} = 0{,}03$}, { $N_{13} = 13$, $Ka_{13} = 0{,}01$; $N_{23} = N_{33} = 21$, $Ka_{23} = Ka_{33} = 0{,}03$}, { $N_{14} = 21$, $Ka_{14} = 0{,}01$; $N_{24} = 21$, $Ka_{24} = 0{,}03$; $N_{34} = 21$, $Ka_{34} = 0{,}1$}, { $N_{15} = 23$, $Ka_{15} = 0{,}01$; $N_{25} = 23$, $Ka_{25} = 0{,}03$; $N_{35} = 23$, $Ka_{35} = 0{,}1$}, { $N_{16} = 25$, $Ka_{16} = 0{,}03$; $N_{26} = N_{36} = 25$, $Ka_{26} = Ka_{36} = 0{,}1$}, { $N_{17} = 27$, $Ka_{17} = 0{,}03$; $N_{27} = N_{37} = 27$, $Ka_{27} = Ka_{37} = 0{,}1$}, where the first subscript indicates the component and the second marks the filter set number.

For algorithms ASWFmed1P and ASWFmed2P (10), noise levels are distinguished using the following thresholds: $\eta_1 = 0{,}001$; $\eta_2 = 0{,}003$; $\eta_3 = 0{,}005$; $\eta_4 = 0{,}02$; $\eta_5 = 0{,}09$; $\eta_6 = 0{,}15$; $\eta_7 = 0{,}2$. Accordingly, filter sets are switched, where each set has two components: a sub-filter weighted FIR median hybrid filter and a simple averaging filter with the following parameters: { $N_{21} = N_{31} = 9$}, { $N_{12} = 9$; $N_{22} = N_{32} = 11$}, { $N_{13} = 13$; $N_{23} = N_{33} = 13$}, { $N_{14} = 15$; $N_{24} = N_{34} = 15$}, { $N_{15} = 17$; $N_{25} = N_{35} = 17$}, { $N_{16} = 19$; $N_{26} = N_{36} = 19$}, { $N_{17} = 21$; $N_{27} = N_{37} = 21$}.

The suggested noise and signal-adapting algorithms for nonstationary noise removal are compared with nonadaptive nonlinear filters, which are effective for EOG signals processing. The reference filters are denoted as follows: Med is a median filter (1), Myr is a myriad filter (2), SWFMH is a sub-filter weighted FIR median hybrid filter (3), SWFMHmyr is the SWFMH algorithm with the median replaced by myriad (4); the number at the end of the filter abbreviation means the sliding window length *N*, for myriad filters the linearity parameter *K* value is specified inside parentheses. All window lengths must be odd.

2. Results and discussion

2.1. Numerical simulations results. The statistical estimates of filtering efficiency for the EOG test signal (Fig. 1, *a*) are presented in Table, statistical estimates of efficiency for EOG test signal according to criteria of MSE ($\times 10^{-8}$) and SNR (sampling frequency f_S = 100 Hz). As can be seen from the numerical simulations results, at the wide range of Gaussian noise variance changing (input SNR lays in the range from 30 to 0 dB) the suggested noise- and signal-adapting myriad algorithms ASWFmyr$_{1P}$, ASWFmyr$_{2P}$ are the most effective. The algorithm ASWFmyr$_{1P}$ (5) prevails over the median ASWFmed$_{1P}$ (10) according to the SNR and MSE criteria: by 3,6–1,5 dB and in 2,3–1,4 times in the range of the input SNR from 35 to 20 dB and by 1,6– 0,8 dB and in 1,4–1,2 times in the range of the input SNR from 15 to 0 dB. On the whole, the algorithm ASWFmyr$_{2P}$ is the most effective, it provides the following indicators of the SNR increase and the MSE decrease due to filtering: by 7,1–10,6 dB and in 5–11,2 times in the wide range of the input SNR from 35 to 10 dB; by 9,1–9,7 dB and in 8–9,3 times at high noise level when the input SNR is in the range from 5 to 0 dB. The selective refiltering increases the filtering efficiency according to the SNR and MSE criteria: by 0,3–0,7 dB and in 1,07–1,17 times in the range of input SNR from 20 to 10 dB and by 0,3 dB and in 1,07 times in the range of input SNR from 5 to 0 dB for the algorithm ASWFmyr$_{2P}$ comparing to ASWFmyr$_{1P}$; by 0,2–0,3 dB and in 1,04–1,08 times when the input SNR belongs to the wide range from 15 to 0 dB for ASWFmed$_{2P}$ comparing to ASWFmed$_{1P}$.

At low noise levels (input SNR lays in the range from 35 to 20 dB), the most effective is the myriad filter with nonlinear properties (linearity parameter K = 0,01, window length N = 13 or 15), its output SNR increases by 7–9,6 dB and the MSE decreases in 5,2–8,4 times. The advantage of the myriad filter over the median with the same window length according to the SNR and MSE criteria is by 3,8–4,6 dB and in 1,5–3 times in the range of the input SNR from 35 to 25 dB and by 3,7 dB and in 2,1 times when the input SNR is 20 dB, however, with noise variance increase the noise suppression by the median filter becomes better. However, in the wide range of the input SNR from 15 to 0 dB, the myriad filter with increased linearity parameter (K = 0,03, N = 17) becomes more effective than the myriad filter with higher nonlinear properties (K = 0,01, N = 17): the improvements of the corresponding output SNR and MSE are by 4,2–1,2 dB and in 2,7–1,3 times, respectively. Compared to the median (N = 17), the myriad filter with increased linearity parameter (K = 0,03) has better efficiency by 3,7–0,3 dB according to SNR and in 2,3–1,1 times according to MSE in the range of the input SNR from 15 to 5 dB, and the median filter performs stronger noise suppression at its very high level (input SNR = 0 dB).

For a wide range from middle to high noise levels (input SNR varies from 15 to 5 dB), the sub-filter weighted FIR myriad hybrid filter (SWFMHmyr) with a larger window length (N = 21) is the most effective among the considered nonadaptive filters, while at high noise levels (input SNRs = 10, 5 dB), the estimates of efficiency for this nonlinear filter are better with increased linearity parameter (K = 0,03). The quantitative assessment shows higher efficiency of the myriad filtering compared to the median. In particular, the myriad algorithm SWFMHmyr (N = 15, K = 0,01) improves the efficiency of the median counterpart SWFMH (N = 15) approximately by 2,2–0,6 dB and in 1,7–1,2 times accordantly to SNR and MSE criteria in a wide range from low to middle noise levels (input SNR belongs to the range from 30 to 10 dB) but loses this advantage at high noise levels (input SNRs = 5,0 dB).

Table

Filter	SNR	MSE	SNR	MSE	SNR	MSE	SNR	MSE
1. Input SNR = 35 dB; NR = 200;			2. SNR = 30 dB;		3. SNR = 25 dB;		4. SNR = 20 dB;	
None	35	211	30	667	25	2108	20	6666
Med13	38,36	97	35,04	209	30,75	562	25,99	1680
Med15	37,50	119	34,56	233	30,5	595	25,83	1742
Myr13(0,01)	42,16	41	39,15	81	34,83	219	29,31	793
Myr15(0,01)	41,31	49	38,93	85	35,06	209	29,55	761
SWFMH13	38,62	92	35,32	196	31,4	483	26,95	1346
SWFFMH15	38,1	103	35,17	203	31,5	472	27,22	1266
SWFMHMyr13(0,01)	40,42	61	37,39	122	33,37	307	28,83	874
SWFMHMyr15(0,01)	40,04	66	37,39	122	33,62	290	29,2	803
ASWFmed1P	38,43	98	36,18	161	32,15	407	27,97	1067
ASWFmed2P	38,43	98	36,12	166	32,0	431	27,99	1064
ASWFmyr1P	42,05	42	39,74	71	35,68	181	29,43	762
ASWFmyr2P	42,05	42	39,61	73	35,72	179	29,72	713
5. SNR = 15 dB;			6. SNR = 10 dB;		7. SNR = 5 dB;		8. SNR = 0 dB	
None	15	21080	10	66662	5	210804	0	666621
Med17	20,79	5569	15,91	17100	11,31	49381	7,79	110943
Med21	20,33	6186	15,5	18806	10,99	53072	7,8	110869
Myr15(0,01)	20,83	5664	14,71	22662	9,95	67578	5,3	197222
Myr17(0,01)	20,28	6432	14,67	22918	10,05	65980	5,47	189674
Myr17(0,03)	24,46	2395	17,66	11511	11,55	46774	6,62	145309
Myr21(0,01)	19,36	7970	14,45	24083	10,12	65011	5,68	180509
Myr21(0,03)	24,41	2427	17,24	12707	11,51	47182	6,81	139064
SWFMH15	22,54	3722	17,74	11240	13,03	33257	8,45	95454
SWFMH17	22,64	3634	17,96	10673	13,29	31319	8,75	88943
SWFMH21	22,78	3523	18,19	10131	13,61	29080	9,18	80561
SWFMHMyr15(0,01)	24,28	2497	18,38	9722	12,28	39506	7,24	126013
SWFMHMyr17(0,01)	24,56	2341	18,85	8740	12,63	36491	7,53	117973
SWFMHMyr17(0,03)	23,52	2965	19,2	8043	13,79	27961	8,5	94376
SWFMHMyr21(0,01)	25,0	2116	19,48	7547	13,17	32278	7,92	107834
SWFMHMyr21(0,03)	23,59	2924	19,53	7444	14,11	25937	8,9	85978
ASWFmed1P	23,27	3147	18,48	9480	13,20	31985	8,64	91235
ASWFmed2P	23,45	3019	18,73	8961	13,48	30036	8,97	84638
ASWFmyr1P	24,88	2175	19,86	6933	13,78	28019	9,43	76113
ASWFmyr2P	25,54	1874	20,55	5949	14,08	26206	9,71	71376

ISSN 2786-6491

Compared to the most effective myriad filter ($N = 15$, $K = 0{,}01$) at low noise levels (input SNR belongs to the range from 35 to 20 dB), the advantage of the algorithm ASWFmyr_{2P} over this nonlinear filter becomes significant when the noise variance increases, namely: ASWFmyr_{2P} prevails in efficiency according to the SNR and MSE indicators by 0,7–0,2 dB and in 1,2–1,1 times at low noise levels (input SNRs = 35, 30, 25, 20 dB), by 4,7–5,8 dB and in 3–3,8 times at middle noise levels (input SNRs = 15, 10 dB), and by 4,1–4,4 dB and in 2,6–2, 8 times at high noise levels (input SNRs = 5, 0 dB). Compared to SWFMHmyr ($N = 17$, $K = 0{,}01$) that provides a high degree of noise suppression in the edges vicinities and has the best performance among the nonadaptive filters at middle-high noise levels (input SNR belongs to the range from 20 to 0 dB), the locally-adaptive myriad algorithm ASWFmyr_{2P} also shows a significant advantage for SNR and MSE criteria, namely: by 3,4–0,4 dB and in 2,2–1,1 times in the range from low to middle noise levels (input SNRs = 35, 30, 20 dB), by 1–2,2 dB and in 1,3–1,7 times at middle-high noise levels (input SNRs = 15, 10, 5, 0 dB). Besides, at high noise levels, the properties linearity for SWFMHmyr should be increased by setting the parameter $K = 0{,}03$. Concerning the most effective nonadaptive filter for each of the simulated cases, the noise- and signal dependent algorithm ASWFmyr_{2P} has an advantage according to the SNR and MSE indicators, as follows: by 0,5–0,7 dB and in 1,11–1,17 times for the input SNR range from 30 to 25 dB, by 0,2, 0,5, and 1 dB and in 1,07, 1,13 and 1,25 times for the input SNRs = 20, 15, 10 dB, respectively, and by 0,5 dB and in 1,13 times for the input SNR = 0 dB. Thus, when the noise variance significantly changes from low to high levels, the application of the suggested noise- and signal-adapting myriad filters is reasonable and much more effective.

2.2. Analysis of signals plots. Significantly more effective filtering in the presence of nonstationary noise in an EOG signal (Fig. 2, *a*) is provided by the proposed noise and signal-adapting myriad algorithms ASWFmyr_{1P}, ASWFmyr_{2P} (5), as can be seen from the plots of output signals, the LAIs and the filter parameters adaptively switched (Fig. 2–4). Visual analysis of the filtering quality confirms the results of numerical evaluations of efficiency (Table). As follows from visual analysis, the suggested real-time noise- and signal-adapting algorithms are mostly correctly choosing the most suitable filter among the given filters for processing the vicinity of the current i-th signal sample depending on the local signal-to-noise situation determined by LAIs. Hence, a high quality of noise filtering and an evident advantage over nonadaptive filters are ensured.

Gaussian noise with different levels of variance is added to the EOG test signal (Fig. 2, *a*): the sections of the test signal, specified by the indices indicated below, correspond to the following values of the input SNR: 35 dB — the indices 1–200; 30 dB — the indices 201–450 and 3201–3450; 25 dB — the indices 451–700 and 2951–3200; 20 dB — the indices 701–950 and 2701–2950; 15 dB — the indices 951–1200 and 2451–2700; 10 dB — the indices 1201–1450 and 2201–2450; 5 dB — the indices 1451–1700 and 1951–2200; 0 dB — the indices 1701–1950.

As is seen (Fig. 2, filtering of a test EOG signal with nonstationary Gaussian noise; *a* — input signal; *b* — output of median filter; *c* — output of myriad filter; *d* — output of sub-filter weighted FIR median hybrid filter; *e* — output of sub-filter weighted FIR myriad hybrid filter *f* — output of one-pass adaptive myriad algorithm ASWFmyr_{1P}; *g* — output of adaptive myriad algorithm ASWFmyr_{2P} with selective re-filtering), all considered nonlinear filters are characterized by high-quality processing of step-like changes: sharp edges are shown to be well-preserved and noise is high-effectively suppressed in their vicinity, at a constant signal a high degree of noise attenuation is provided, as well. At a low noise level, the step edges are clearer depicted in the output signals of the myriad (Myr) filter (Fig. 2, *c*) and the sub-filter weighted FIR

myriad hybrid (SWFMHmyr) filter (Fig. 2, *e*), compared to the median (Med) filter (Fig. 2, *b*) and the sub-filter weighted FIR median hybrid (SWFMH) filter (Fig. 2, *d*), however, the median filter is more effective on the signal part with a very high noise level. Compared to the nonadaptive filters (Fig. 2, *b*–*e*), the enhanced quality of output signals is observed for the locally-adaptive algorithms ASWFmyr$_{1P}$ (Fig. 2, *f*) and ASWFmyr$_{2P}$ (Fig. 2, *g*), while the algorithm ASWFmyr$_{2P}$ with selective re-filtering is the most effective.

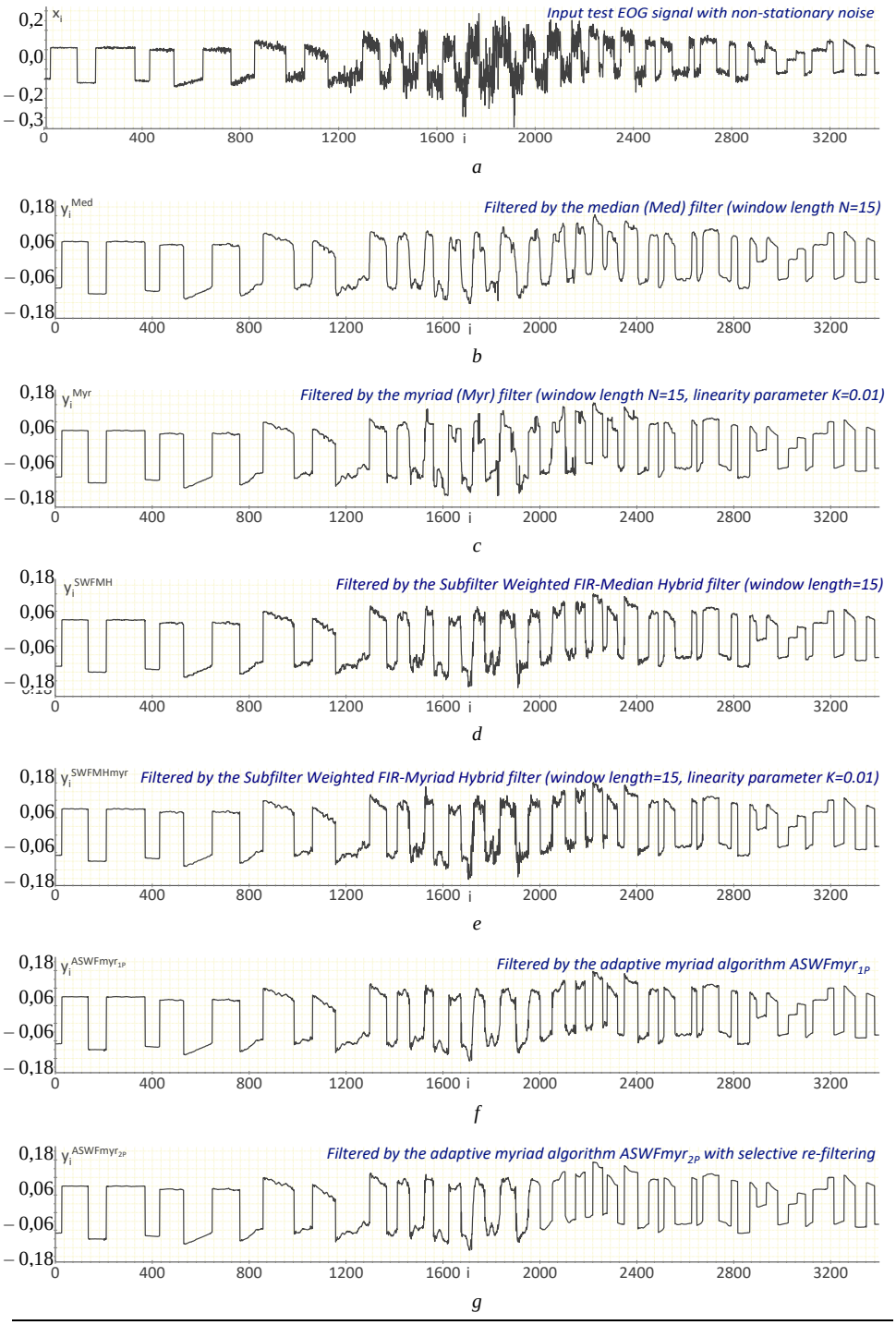

Fig. 2

 ISSN 2786-6491

Similar conclusions follow from the visual analysis of residual noise plots at the filter outputs (Fig. 3, Residual noise after filtering: *a* — simulated nonstationary noise; *b* — residual noise after median filter; *c* — residual noise after myriad filter; *d* — residual noise after sub-filter weighted FIR median hybrid filter; *e* — residual noise after sub-filter weighted FIR myriad hybrid filter; *f* — residual noise after adaptive myriad algorithm ASWFmyr$_{1P}$; *g* — residual noise after adaptive myriad algorithm ASWFmyr$_{2P}$ with selective re-filtering). As can be seen, at the signal parts with low and middle noise levels, the algorithms with the utilization of myriad filtering Myr (Fig. 3, *c*) and SWFMHmyr (Fig. 3, *e*) suppress noise better as compared to the median filters Med (Fig. 3, *b*) and SWFMH (Fig. 3, *d*), however, at the very noisy signal part, the residual noise amplitude deviation after median filter applying is smaller. The residual noise plots for the noise- and signal-dependent algorithms ASWFmyr$_{1P}$ and ASWFmyr$_{2P}$ (Fig. 3, *f*, *g*) demonstrate a significant attenuation of noise power compared to the non-adaptive filters (Fig. 3, *b*–*e*) and the usefulness of selective re-filtering for the locally-adaptive algorithm ASWFmyr$_{2P}$ (Fig. 3, *f*, *g*). As a result of median filtering (Fig. 3, *b*), at the signal part with a high noise level, the maximum absolute deviation of the residual noise is lower than for other filters (Fig. 3, *c*–*g*), however, on the whole, the quality of nonstationary noise suppression for the noise- and signal-adapting myriad algorithms (Fig. 3, *f*, *g*) is noticeably better.

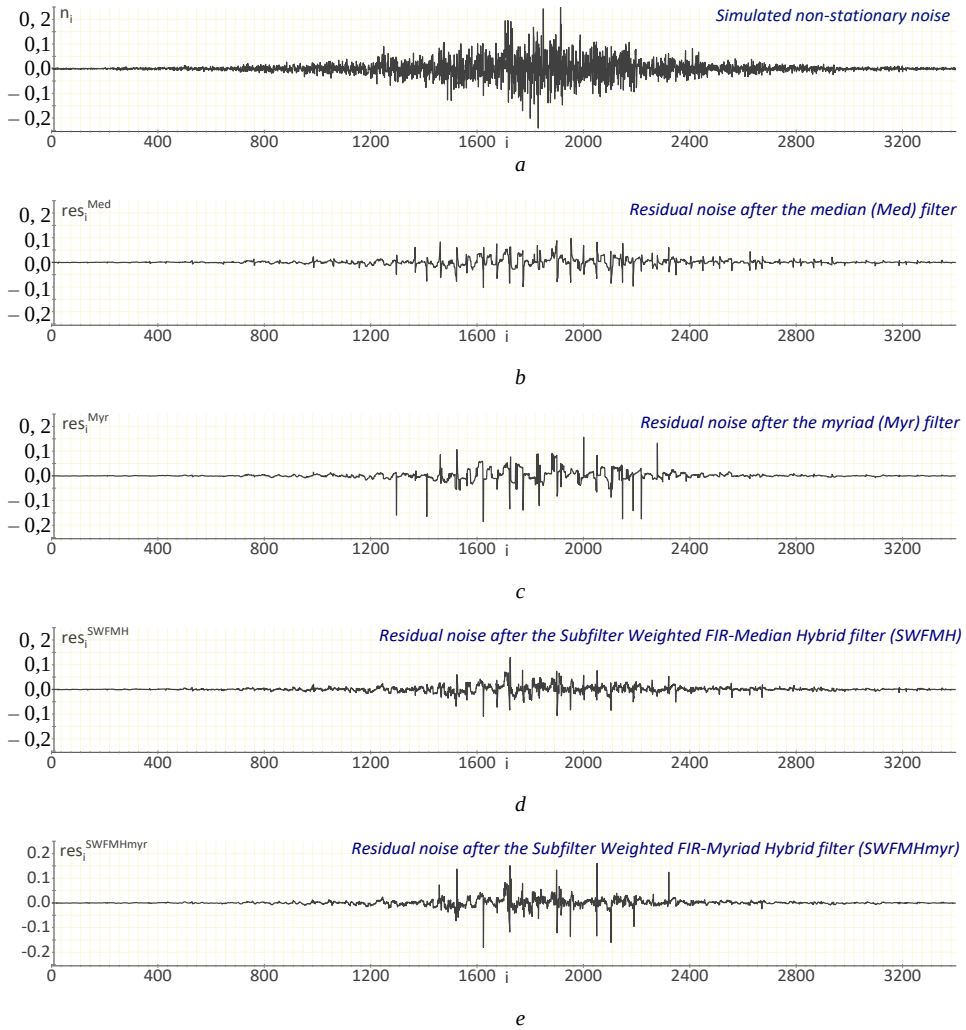

a

b

c

d

e

Fig. 3

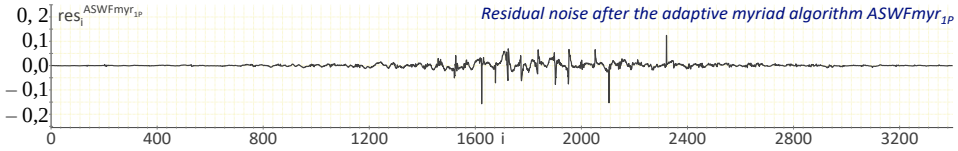

f

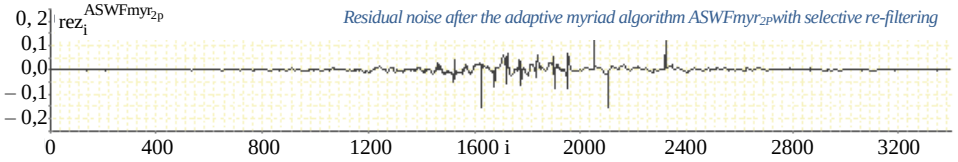

g

The behavior of LAIs and filter parameters adaptable during signal processing for the proposed locally-adaptive myriad algorithm (5) (Fig. 4, local activity indicators and adaptable filter parameters: *a*) input signal; *b*) smoothed Hampel parameters r_i^f, th_i^f; *c* — filtered absolute value of *Z*-parameter quasi-range $|Q_{Z_i}^f|$; *d* — noise level estimation by flag variable, number of re-filtering; *e* — filter switching depending on noise level estimation and LAIs comparison (*y*-axis is offset for illustration of IPF and NSF by 10 and 20 units; *e*) adaptable algorithm's parameters switching: window length, linearity parameter of myriad filter Ka (multiplied by 100)) clearly illustrates the idea of locally-adaptive nonlinear filtering with «hard» switching of parameters' values. The condition for Hampel parameters comparison $th_i^f > r_i^f$ (Fig. 4, *b*) and close to unity *Z*-parameter quasi-range $|Q_{Z_i}^f|$ values (Fig. 4, *c*) correctly determine edges and, accordingly, switch the nonlinear filters with high dynamical properties for processing, in this case, Myr or SWFMHmyr filters with a small linearity parameter value (Ka = 0,01). At the constant signal parts, filters with linear properties ensuring high-effective noise suppression are mainly used, in this case, Myr (at a low noise level) and SWFMHmyr (at higher noise levels) with linearity parameter Ka = 0,03 for Myr and Ka = 0,1 for SWFMHmyr (Fig. 4, *d*). The flag $\hat{n}_i$ (9) is tracking noise level changes (Fig. 4, *e*) and, relatively, filter sets with more appropriate window length settings increasing by the noise variance increase are being switched. For the entire signal, except its beginning with a very low noise level, the flag $\hat{n}_i$ is greater than 2, therefore the locally-adaptive algorithm ASWFmyr$_{2P}$ performs re-filtering. The window length N and the linearity parameter Ka are switched to smaller values, ensuring the myriad filter high nonlinearity mode in the vicinity of the edges, and to larger values, ensuring linear, close to averaging, myriad filter properties at the constant signal segments (Fig. 4, *f*). The filter window length for processing the current sample is enlarged when the noise level increases and is diminished otherwise (Fig. 4, *f*).

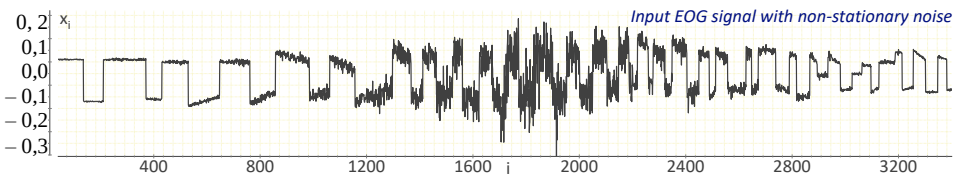

a

Fig. 4

 ISSN 2786-6491

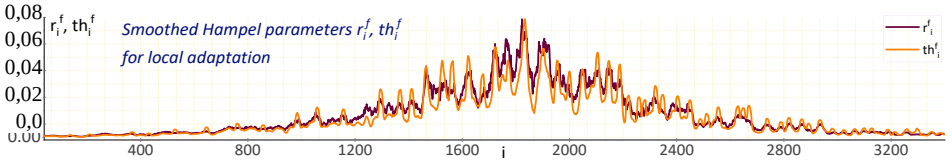

b

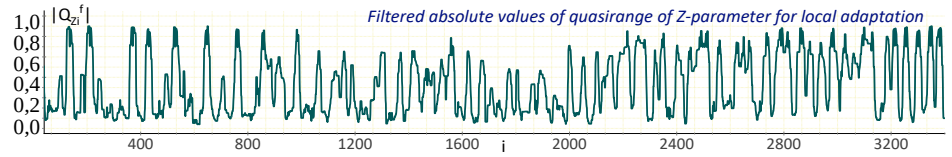

c

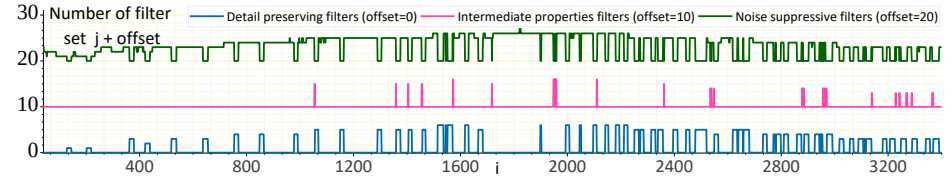

d

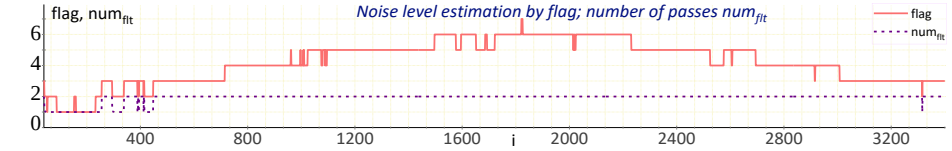

e

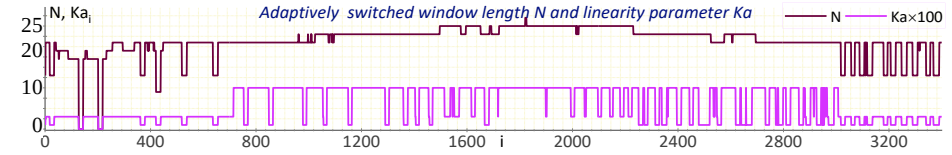

f

Conclusion

This paper introduced new noise- and signal-adapting real-time filtering algorithms for nonstationary noise (with time-varying variance) removal in the electrooculographic biomedical signals. During the sample-by-sample signal processing in these algorithms the selection of the filter set and parameters is determined based on the local estimates of the noise level and signal behavior. This is achieved through the comparison of the local activity indicators calculated for each signal sample. By analyzing the LAIs, a filter set with the most suitable window length settings and a filter with appropriate parameters are being automatically selected during a signal processing to process a vicinity of the current sample. One of the proposed algorithms involves adaptive switching of myriad and FIR hybrid filters with a proposed extension to replace median operation by myriad with high edges processing quality taking into account. The algorithm chooses the most suitable values of window length and linearity parameter controlling myriad filter nonlinearity for local signal processing from the fixed set of relevant values. An alternative algorithm is proposed to address scenarios with significant computational complexity limitations during signal processing. This algorithm performs adaptive

switching between sub-filter weighted FIR median hybrid filters for high-edge filtering quality and simple averaging filters for effective noise suppression in linear signal sections. The advantages of such locally-adaptive algorithms include their independence from prior knowledge about the local signal behavior model and noise variance. These algorithms also eliminate the need for time-consuming adjustments and precise tuning of filter parameters during signal processing. Moreover, they can be implemented with low computational complexity, enabling real-time processing.

The statistical estimates of filtering efficiency evaluated by numerical simulations for the EOG model signals and the output signals plots show the high quality of nonstationary noise suppression by the proposed noise- and signal-adapting algorithms, as well as the expediency of selective re-filtering depending on the noise level preliminary assessment. A significant advantage is demonstrated in the effectiveness of the proposed locally-adaptive nonlinear filtering algorithms compared to the reference filters, which are effective for the specified signals. For all simulated situations of the input SNR wide range from 35 to 0 dB, the proposed locally-adaptive algorithm based on the myriad and the sub-filter weighted FIR myriad hybrid filters demonstrates the best efficiency indicators: in the wide range of input SNR changes from 35 to 10 dB, they provide the SNR increase by 7,1–10,6 dB while the corresponding MSE decrease in 5–11,2 times, and at high noise levels when input SNR varies from 5 to 0 dB, the SNR increases by 9,1–9,7 dB and the MSE decreases 8–9,3 times. The locally-adaptive algorithm based on sub-filter weighted FIR median hybrid filters and averaging filters require simpler calculations, however, it inferiors in noise suppression efficiency compared to the adaptive myriad algorithm which also allows real-time implementation with the utilization of high-speed computers. The advantage of the locally-adaptive myriad algorithm over the well-known median filter is 5–3 dB. The analysis of the filter output signals plots, the LAIs, and filter parameters, which during signal processing adapt to the changes in local signal behavior and noise level, is confirmed with the calculated statistical estimates of the filters' efficiency. The high quality of nonstationary noise attenuation and the noticeable advantages over nonadaptive nonlinear filters are shown.

Н.О. Тулякова, О.М. Трофимчук

АЛГОРИТМИ АДАПТИВНОЇ МІРІАДНОЇ ФІЛЬТРАЦІЇ ДЛЯ УСУНЕННЯ НЕСТАЦІОНАРНОГО ШУМУ В ЕЛЕКТРООКУЛОГРАМАХ

Тулякова Наталія Олегівна

Інститут прикладної фізики НАН України, Суми,

nataliyatulyakova@google.com

Трофимчук Олександр Миколайович

Інститут телекомунікацій та глобального інформаційного простору НАН України, Київ,

trofymchuk@nas.gov.ua

Усунення в біомедичних сигналах нестаціонарного шуму важливо для забезпечення високоякісної діагностики. Нестаціонарний шум складно видалити через його змінні в часі й апріорно невідомі характеристики. Застосування лінійної фільтрації до електроокулографічних (ЕОГ) сигналів приводить до згладжування діагностично важливих різких змін сигналу, викликаних сакадичними рухами очей. З цієї причини для

обробки перепадів та інших точок розриву похідної більш доцільними є нелінійні фільтри на основі робастних оцінок. У статті представлено адаптивні алгоритми нелінійної фільтрації нестаціонарного шуму в реальному часі в сигналі ЕОГ за допомогою шумо- та сигнал-залежного перемикання фільтру, більш придатного для обробки локального околу поточного відліку вхідного сигналу. Один із алгоритмів базується на міріадних і зважених КІХ (кінцева імпульсна характеристика)-гібридних міріадних фільтрах. У ньому пропонується замінити медіанну операцію міріадою з адаптивним перемиканням довжини вікна та значень параметру лінійності. Інший алгоритм адаптивно перемикає зважені КІХ-гібридні медіанні фільтри та фільтри усереднення з різною довжиною вікна, забезпечуючи простіші обчислення та високу швидкодію. Ці алгоритми не потребують часу для модифікації параметрів та їхнього точного налаштування під час обробки сигналу, попереднього знання моделі сигналу та дисперсії шуму. Проведено чисельне моделювання для оцінки якості фільтрації за критеріями середньоквадратичної похибки та співвідношення сигнал/шум для модельного сигналу при різних рівнях гаусова шуму. Отримані результати свідчать про високу якість заглушування нестаціонарного шуму в ЕОГ. Адаптивний алгоритм міріадного типу перевершує медіанний за ефективністю, проте вимагає чисельного методу для мінімізації функції вартості, однак їх реалізація в реальному часі можлива з використанням високошвидкісних комп'ютерів. Запропоновані адаптивні алгоритми значно покращують ефективність неадаптивних фільтрів.

Ключові слова: електроокулографічні сигнали, нестаціонарний шум, адаптивна фільтрація в реальному часі.

REFERENCES

1. Berg P., Scherg M. Dipole models of eye movements and blinks. *Electroeceph. and Clin. Neurophysiol.* 1991. N 79. P. 36–44.
2. Bahill A.T., Brockenbrough A., Troost B.T. Variability and development of a normative data base for saccadic eye movements. *Investigative Ophthalmology & Visual Science.* 1981. Vol. 21, N 1. P. 116–125.
3. Sweeney K.T., Ward T.E., McLoone S.F. Artifact removal in physiological signals — practices and possibilities. *IEEE Transactions on Information Technology in Biomedicine.* 2012. Vol. 16, N 3. P. 488–500. DOI: https://doi.org/10.1109/TITB.2012.2188536.
4. Jiang X., Bian G.-B., Tian Z. Removal of artifacts from EEG signals: a review. *Sensors.* 2019. Vol. 19, N 5. 987 p. DOI: https://doi.org/10.3390/s19050987.
5. Nodes T., Gallagher N. Median filters: some modifications and their properties. *Proc. of the IEEE Transactions on Acoustics. Speech, and Signal Processing.* 1982. Vol. 30, N 5. P. 739–746.
6. Juhola M. Median filtering is appropriate to signals of saccadic eye movements. *Computers in biology and medicine*. 1991. Vol. 21, N 1-2. P. 43–49.
7. Astola J., Heinonen P., Neuvo Y. On root structures of median and median-type filters. *Proc. of the IEEE Transactions on Acoustics, Speech, and Signal Processing.* 1987. Vol. 35, N 8. P. 1199–1201.
8. Heinonen P., Neuvo Y. FIR-median hybrid filters. *Proc. of the IEEE Transactions on Acoustics, Speech, and Signal Processing.* 1987. Vol. 35, N 6. P. 832–838.
9. Heinonen P., Neuvo Y. Median type filters with predictive FIR substructures. *Proc. of the IEEE Transactions on Acoustics, Speech, and Signal Processing*. 1988. Vol. 36, N 6. P. 892–899.
10. Nieminen A., Heinonen P., Neuvo Y. A new class of detail-preserving filters for image processing. *IEEE Trans Pattern Analysis and Machine Intelligens PAMI-9*. 1987. P. 74–90.
11. Neejarvi J., Varri A., Fotopouls S., Neuvo Y. Weighted FMH filters. *Signal Processing*. 1993. N 31. P. 181–190.
12. Kalluri S., Arce G.R. Adaptive weighted myriad filter algorithms for robust signal processing in α-stable noise environments. *Proc. of the IEEE Transactions on Signal Processing.* 1998. N 46. P. 322–334. DOI: https://doi.org/10.1109/78.655418.

13. Gonzalez J.G., Arce G.R. Optimality of the myriad filter in practical impulsive-noise environments. *Proc. of the IEEE Transactions on Signal Processing*. 2001. Vol. 49, N 2. P. 438–441. DOI: https://doi.org/10.1109/78.902126.
14. Gonzalez J.G., Arce G.R. Statistically-efficient filtering in impulsive environments: weighted myriad filters. *EURASIP Journal on Advances in Signal Processing*. 2002. N 363195. P. 4–20. DOI: https://doi.org/10.1155/S1110865702000483.
15. Pander T. An application of weighted myriad filter to suppression an impulsive type of noise in biomedical signals. *TASK Quartarly*. 2004. Vol. 2, N 8. P. 199–216.
16. Carrillo R.E., Aysal T.C., Barner K.E. A generalized Cauchy distribution framework for problems requiring robust behavior. *EURASIP Journal on Advances in Signal Processing*. 2010. N 312989. P. 19. DOI: https://doi.org/10.1155/2010/312989.
17. Astola J., Kuosmanen P. Fundamentals of nonlinear digital filtering. New York : CRC Press, 1997. P. 276.
18. Pitas I., Venetsanopoulos A.N. Nonlinear digital filters: principles and application. USA : Kluwer Academic Publ., 1990. P. 324. DOI: https://doi.org/10.1007/978-1-4757-6017-0.
19. Bovic A., Huang T., Munson D. A generalization of median filtering using linear combinations of order statistics. *IEEE Transactions on Acoustics, Speech, and Signal Processing*. 1983. Vol. 31, N 6. P. 1342–1350. DOI: https://doi.org/10.1109/TASSP.1983.1164247.
20. Bernstein R. Adaptive nonlinear filters for simultaneous removal of different kinds of noise in images. *Proc. of the IEEE Transactions On Circuits and Systems.* 1987. Vol. 34, N 11. P. 1275–1291. DOI: https://doi.org/10.1109/TCS.1987.1086066.
21. Melnik V.P., Lukin V.V., Zelensky A.A., Astola J.T., Kuosmanen P. Local activity indicators for hard-switching adaptive filtering of images with mixed noise. *Optical Engineering.* 2001. Vol. 40, N 8. P. 1441–1455. DOI: https://doi.org/10.1117/1.1385815.
22. Lukin V.V., Zelensky A.A., Tulyakova N.O., Melnik V.P., Peltonen S., Kuosmanen P. Locally-adaptive processing of 1-D signals using Z-parameters and filter banks. NORSIG'2000: *Proc. of the Nordic Signal Processing Symposium.* 2000. P. 195–197.
23. Tulyakova N.O., Trofimchuk A.N. Locally adaptive filtering of nonstationary noise in long-term electrocardiographic signals. *Radioelectronic and Computer Systems*. 2020. Vol. 4, N 96. P. 16–33. DOI: https://doi.org/10.32620/reks.2020.4.02.
24. Tulyakova N., Trofymchuk O. Real-time filtering adaptive algorithms for nonstationary noise in electrocardiograms. *Biomedical Signal Processing and Control*. 2022. Vol. 72, Part A. P. 103308. DOI: https://doi.org/10.1016/j.bspc.2021.103308.
25. Tulyakova N., Trofymchuk O. Adaptive myriad filter with time-varying noise- and signal-dependent parameters. *Radioelectronic and Computer Systems*. 2022. Vol. 2, N 102. P. 217–238. DOI: https://doi.org/10.32620/reks.2022.2.17.
26. Bortolan G., Christov I. Dynamic filtration of high-frequency noise in ECG signal. *Computing in Cardiology*. 2014. N 41. P. 1089–1092.
27. Christov I., Neycheva T., Schmid R., Stoyanov T., Abächerli R. Pseudo-real-time low-pass filter in ECG, self-adjustable to the frequency spectra of the waves. *Medical & Biological Engineering & Computing*. 2017. N 55. P. 1579–1588. DOI: https://doi.org/10.1007/s11517-017-1625-y.
28. Christov I., Neycheva T., Schmid R. Fine tuning of the dynamic low-pass filter for electromyographic noise suppression in electrocardiograms. *Computing in Cardiology*. 2017. N 44. P. 1–4. https://doi.org/10.22489/CinC.2017.088-007.
29. Christov I., Raikova R., Angelova S. Separation of electrocardiographic from electromyographic signals using dynamic filtration. *Medical Engineering and Physics*. 2018. N 57. P. 1–10. DOI: https://doi.org/10.1016/j.medengphy.2018.04.007.
30. Savitzky A., Golay M. Smoothing and differentiation of data by simplified least squares procedures. *Analytical Chemistry*. 1964. N 36. P. 1627–1639. DOI: https://doi.org/10.1021/ac60214a047.
31. Christov I.I., Daskalov I.K. Filtering of electromyogram artifacts from the electrocardiogram. *Medical Engineering & Physics*. 1999. N 21. P. 731–736. DOI: https://doi.org/10.1016/S1350-4533(99)00098-3.
32. Bortolan G., Christov I., Simova I., Dotsinsky I. Noise processing in exercise ECG stress test for the analysis and the clinical characterization of QRS and T wave alternans. *Biomedical Signal Processing and Control*. 2015. N 18. P. 378–385. DOI: https://doi.org/10.1016/j.bspc.2015.02.003.
33. Christov I., Gotchev A., Bortolan G., Neycheva T., Raikova R., Schmid R. Separation of the electromyographic from the electrocardiographic signals and vice versa. A topical review of

the dynamic procedure. *Int. J. Bioautomation*. 2020. Vol. 24, N 3. P. 289–317. DOI: https:// doi.org/10.7546/ijba.2020.24.3.000744.
34. Tulyakova N., Neycheva T., Trofymchuk O., Stryzhak O. Locally-adaptive myriad filtration of one-dimensional complex signal. *Int. J. Bioautomation*. 2018. Vol. 22, N 3. P. 273–294.
35. Tulyakova N. Locally-adaptive myriad filters for processing ECG signals in real time. *Int. J. Bioautomation.* 2017. Vol. 21, N 1. P. 5–18.
36. Tulyakova N., Trofimchuk A., Strizhak A. Adaptive algorithms for elimination of electromyographic noise in the electrocardiogram signal. *Telecommunications and Radio Engineering*. 2018. Vol. 77, N 6. P. 549–561. DOI: https://doi.org/10.1615/TelecomRadEng.v77.i6.70.
37. Abramov S., Lukin V., Astola J. Myriad filter properties and parameter selection. UkrOBRAZ'2000: *Proc. of the Fifth All-Ukrainian Int. Conf*. 2000. P. 59–62.
38. Tulyakova N., Trofymchuk O. Modified algorithms for signal nonlinear trend detection. *Radiotekhnika*. 2021. Vol. 206. P. 135–149. DOI: https://doi.org/10.30837/rt.2021.3.206.13.
39. Yuriy S.S., Yrjö N., Sanowar K. Review of unbiased FIR filters, smoothers, and predictors for polynomial signals. *Frontiers in Signal Processing*. 2018. Vol. 2, N 1. DOI: https: // dx.doi.org/10.22606/fsp.2018.21001.
40. Davies L., Gather U. The identification of multiple outliers. *J. American Statistical Association* 1993. N 88. P. 782–801. DOI: https://doi.org/10.1080/01621459.1993.10476339.
41. Pearson R.K., Neuvo Y., Astola J., Gabbouj M. The class of generalized Hampel filters. EUSIPCO'2015: *Proc. of the 23rd European Signal Processing Conference*. 2015. P. 2501–2505. DOI: https://doi.org/10.1109/EUSIPCO.2015.7362835.
42. Wichman R., Astola J., Heinonen P., Neuvo Y. FIR-median hybrid filters with excellent transient response in noisy conditions. *Proc. of the IEEE Transactions on Acoustics, Speech and Signal Processing*. 1990. Vol. 38, N 12. P. 2108–2117.
43. Neejarvi J., Neuvo Y., Varri A., Mitra U. Algorithms for real-time trend detection. *Signal Processing*. 1989. N 18. P. 1–15.
44. Pander T., Czabański R., Przybyła T., Pojda-Wilczek D. An automatic saccadic eye movement detection in an optokinetic nystagmus signal. *Biomedizinische Technik. Biomedical Engineering*. 2014. Vol. 59, N 6. P. 529–543. DOI: https://doi.org/10.1515/bmt-2013-0137.
45. Abramov S.K. Myriad filtering realization algorithm. *Aerospace Technique and Technology*. 2000. N 21. P. 143–147.
46. Tulyakova N.O., Trofimchuk A.N., Strizhak A.E. Algorithms of myriad filtering. *Radioelectronic and Computer Systems*. 2014. Vol. 4, N 68. P. 76–83.

Submitted 05.07.2023